

Correlation between wearable inertial sensor data and standardised Parkinson's disease axial impairment measures using machine learning

Original

Correlation between wearable inertial sensor data and standardised Parkinson's disease axial impairment measures using machine learning / Borzi', L.; Manoni, A.; Zampogna, A.; Irrera, F.; Suppa, A.; Olmo, G.. - ELETTRONICO. - 2022:(2022), pp. 732-736. (Intervento presentato al convegno IEEE 21st Mediterranean Electrotechnical Conference (MELECON) tenutosi a Palermo nel 14-16 June 2022) [10.1109/MELECON53508.2022.9843018].

Availability:

This version is available at: 11583/2971866 since: 2022-09-30T06:54:02Z

Publisher:

IEEE

Published

DOI:10.1109/MELECON53508.2022.9843018

Terms of use:

This article is made available under terms and conditions as specified in the corresponding bibliographic description in the repository

Publisher copyright

IEEE postprint/Author's Accepted Manuscript

©2022 IEEE. Personal use of this material is permitted. Permission from IEEE must be obtained for all other uses, in any current or future media, including reprinting/republishing this material for advertising or promotional purposes, creating new collecting works, for resale or lists, or reuse of any copyrighted component of this work in other works.

(Article begins on next page)

Correlation between wearable inertial sensor data and standardised Parkinson's disease axial impairment measures using machine learning

Luigi Borzi*

*Dept. Control and Computer Engineering
Politecnico di Torino
Turin, Italy
luigi.borzi@polito.it*

Alessandro Manoni

*Dept. Information Engineering, Electronics and Telecommunication
Sapienza University
Rome, Italy
alessandro.manoni@uniroma1.it*

Alessandro Zampogna

*Dept. Human Neurosciences
Sapienza University
Rome, Italy
alessandro.zampogna@uniroma1.it*

Fernanda Irrera

*Dept. Information Engineering, Electronics and Telecommunication
Sapienza University
Rome, Italy
fernanda.irrera@uniroma1.it*

Antonio Suppa

*Dept. Human Neurosciences
Sapienza University
Rome, Italy
IRCCS NEUROMED Institute
Pozzilli, Italy
antonio.suppa@uniroma1.it*

Gabriella Olmo

*Dept. Control and Computer Engineering
Politecnico di Torino
Turin, Italy
gabriella.olmo@polito.it*

Abstract—Wearable sensors represent a valuable means for monitoring motion signs and symptoms of Parkinson's disease (PD). In this paper, we explore the potential of a single inertial sensor to yield information correlated to the patient's subjective perception of axial motion impairment during daily activities. This latter is expressed using as a relevant metric the sum of MDS-UPDRS items 2.11-2.13. **Methods:** thirty-one patients with PD were enrolled in this study, and asked to perform a timed-up-and-go test while wearing an inertial sensor on their thigh. Several time- and frequency-domain features were extracted from the inertial signals. They were fed to a random forest regression model for the prediction of the axial impairment metric. The model was optimized using 10-fold cross-validation and performance were assessed using leave-one-subject-out test. **Results:** Pearson correlation coefficient with the addressed metric of 0.76 (0.86) and mean absolute error of 1.70 (1.52) were obtained in patients under (not under) dopaminergic therapy. Moreover, moderate to strong correlations were found between the predicted score and some important disease progression, axial impairment, and motor performance metrics. **Conclusion:** a single wearable inertial sensor may be used for assessing motor disabilities of patients with PD.

Index Terms—Parkinson's disease, UPDRS, wearable inertial sensors, gait, prediction, machine learning, random forest

I. INTRODUCTION

Parkinson's disease (PD) is one of the most common neurodegenerative disorders, affecting more than 1% of individuals over the age of 60 [1]. Cardinal PD motor signs

include rigidity, tremor at rest, bradykinesia (i.e. slowness of movement) and postural instability [2], [3]. As a result, a reduction in the quality of life and an increase in the risk of falls in the PD population are observed [4].

The Movement Disorder Society - Unified Parkinson's Disease Rating Scale (MDS-UPDRS) [5] is one of the most used clinical rating scales, and evaluates various aspects of the disease, including non-motor and motor experiences of daily living and motor complications. The scale encompasses six parts. Part I aims at assessing mental state, behavior, mood, pain and autonomic functions. Part II is a patient self-evaluation of several motor aspects of daily activities, as perceived in the days preceding the interview. Part III is the clinical evaluation of several motor skills. Part IV scores possible complications such as dyskinesia (i.e. involuntary movements) and fluctuations of several clinical conditions; finally, part V and VI take into account the severity of the disease (Hoehn and Yahr scale - H&Y) and the disability degree. A score between 0 and 4 is assigned to each item, according to the severity of the symptom at hand, and following proper guidelines.

The clinical evaluation, performed only within pre-scheduled follow-up sessions, makes difficult for clinicians to appreciate short-term variations of the patient's disability level and to plan proper therapy adjustments. Moreover, it is not

always indicative of the patient’s perception of their impairment during daily activities. In fact, these latter are typically self-evaluated by the patients themselves and reported in the medical history via the MDS-UPDRS Part II.

Wearable technology has been widely used to assess PD motor disorders. The combination of inertial sensors and machine learning (ML) techniques has been successfully employed for the monitoring of specific motor aspects, including postural stability [6], bradykinesia [7], dyskinesia [8], tremor [9], and freezing of gait (i.e., a sudden motor block) [10], [11]. Some authors investigated the use of inertial sensors to predict specific UPDRS items [12]–[15].

In [13], 75 PDPs were equipped with a smartphone positioned on lower back. Inertial data during turning was analyzed, and time- and frequency-domain features were extracted and fed to a linear discriminant analysis classifier. The model output correlated with the UPDRS gait ($r = 0.61$, $p < 0.001$) and postural stability ($r = 0.72$, $p < 0.001$) score. In [14], inertial data from 75 patients with PD (PDPs) were recorded during gait using a single inertial measurement unit (IMU) on the waist. A support vector machine classifier was employed for gait detection, and the power spectra in the 0–10 Hz range was computed and used as output. The algorithm output correlated with the UPDRS gait ($r = 0.73$, $p < 0.001$) and postural stability ($r = 0.42$, $p < 0.001$) score. Recently, in [16], 31 PDPs were equipped with 3 inertial sensors on the lower back and on each foot. Inertial data related to gait, turn, and stance activities were analysed. The output of a multivariate linear regression model correlated with the total UPDRS-part III ($r = 0.48$, $p = 0.007$).

In [17], we used a single inertial sensor to estimate the axial motor impairment of PDPs, clinically evaluated by means of the postural stability and gait difficulty (PIGD) score. On the other hand, in this study, we aim to establish the usefulness of motion data taken using a single inertial sensor for the prediction of axial impairment as self-reported by the patients themselves during daily activities. These latter are related to the sum of MDS-UPDRS items 2.11-2.13, taken as the reference metric to evaluate the performance of the proposed algorithm.

II. MATERIALS AND METHODS

This section describes the participants enrolled in this study (sec. II-A), the data acquisition procedures (sec. II-B), the preprocessing steps (sec. II-C), the implementation and optimization of the prediction model (sec. II-D), and finally the performance evaluation procedures (sec. II-E).

A. Participants

Thirty-one PDPs were enrolled from the Movement Disorder outpatient clinic of the Department of Human Neuroscience, Sapienza University of Rome, Italy. Inclusion criteria were: diagnosis of idiopathic PD; lack of dementia (i.e. Mini-Mental State Examination—MMSE > 24); ability to walk autonomously; lack of neurological or orthopaedic comorbidities possibly affecting gait. PDPs were clinically assessed in

both OFF (i.e. after L-Dopa withdrawal for at least 12 h) and ON (1 h after L-Dopa intake) state of therapy. In addition, L-Dopa equivalent daily dose (LEDD) was calculated for each patient. The following standardised scales for clinical assessment were used: H&Y, modified MDS-UPDRS part III, MMSE. In order to further assess axial impairment, the PIGD score was calculated, in both OFF and ON state of therapy. Finally, the sum of MDS-UPDRS items 2.11-2.13 (getting out of bed, car, or deep chair; walking and balance; freezing of gait) was computed and addressed as the reference axial impairment metric (AIM), as it is representative of the self-perceived status during the several days preceding the MDS-UPDRS interview. Demographic and clinical features of PDPs enrolled in this study are summarized in Tab.I. Experimental procedures were approved by the institutional review board and performed according to the Declaration of Helsinki.

TABLE I
DEMOGRAPHIC AND CLINICAL FEATURES OF PATIENTS ENROLLED IN THE PRESENT STUDY. H&Y: HOEHN AND YAHR SCALE. MMSE: MINI-MENTAL STATE EXAMINATION. LEDD: L-DOPA EQUIVALENT DAILY DOSE. PIGD: POSTURAL STABILITY AND GAIT DIFFICULTY SCORE

Feature	Mean value	Range
Age (years)	71.9	57-84
Disease duration (years)	10.9	2-23
H&Y	2.4	1-4
MMSE	28.1	24-30
LEDD (mg)	819	300-2296
MDS-UPDRS III OFF	35.9	12-68
MDS-UPDRS III ON	27.9	7-64
PIGD OFF	7.3	0-18
PIGD ON	6.4	0-15
MDS-UPDRS 2.11-2.13	4.9	0-12

B. Data acquisition

PDPs performed a 7-m timed-up-and-go test, consisting of getting up from a chair, walking back and forth for 7 meters, and finally sitting down. Patients’ gait was video-recorded through a camera and monitored by a single IMU placed and fixed on the thigh through an elastic band. The IMU was positioned on patients’ thigh so that when they were standing, the y-axis represented the inverse gravity vector and x-axis lies in the frontal plane. Hence, the angular velocity around the x-axis allowed a good representation of the thigh motion during linear gait. The STMicroelectronics system-on-board prototype nMEMSi [18] was employed. It is equipped with a 9-axis IMU (LSM9DS0), integrating a 3-axis accelerometer and a 3-axis gyroscope; a Bluetooth V3.0 module (BT33); a lithium-ion battery; an ultralow-power 32-bit microcontroller (STM32L1). Sensors range was settable up to ± 16 g and ± 2000 dps for accelerometer and gyroscope, respectively, and sample frequency up to 200 Hz. The device size (including battery) is 25 mm \times 30 mm \times 4 mm. For the aim of the present experiments, the range was set to ± 2 g and ± 245 dps for accelerometer and gyroscope, respectively, with a sensitivity of 61 μ g/LSB and 8.75 mdps/digit. The sample frequency was set to 60 Hz. Data recorded during the experiments were

transmitted in real-time to a personal computer through the neMEMSi Bluetooth module and progressively saved in CSV format. Data in CSV files were processed offline as described in the next section.

C. Preprocessing

Raw readings from accelerometer and gyroscope were fused using a Kalman filter [19] to estimate the sensor orientation. The sensor fusion algorithm iteratively integrates the gyroscope readings to obtain an orientation estimate, and corrects the generated slow-varying bias using the accelerometer readings. In order to remove low-frequency trends and high frequency noise, orientation, acceleration, and angular velocity signals were filtered using a second-order zero-lag band-pass Butterworth filter, with cutoff frequencies of 0.5 Hz and 20 Hz. The orientation signal was further low-pass filtered using a second-order zero-lag Butterworth filter, with a cut-off frequency of 2 Hz. In order to select only the walking segments of data, a continuous wavelet transform (CWT) approach was implemented. A Morse mother wavelet was employed, due to its similarity with the orientation signal pattern during walking. The CWT analysis was performed in the frequency range 0.5–2 Hz, as stride time in PDPs was found to range from 0.71 s to 1.55 s [20]. The time-frequency representation of the orientation signal, restricted in the 0-1 Hz range, and the resulting walking bouts detection are reported in Fig.1.

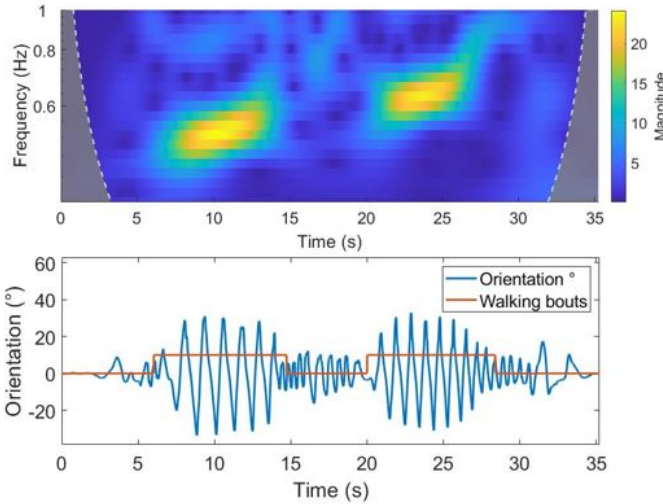


Fig. 1. Time-frequency representation of orientation signal based on Continuous Wavelet Transform (top); orientation signal and walking detection output (bottom).

In each walking segment, initial contacts (ICs) were identified as the positive orientation signal peaks [21]. Only peaks exceeding the signal standard deviation and at least 0.5 s apart were selected. Final contacts (FCs) were identified as the negative peaks following the ICs [21]. The acceleration, angular velocity, and orientation recordings were segmented into windows corresponding to strides (i.e. from an IC to the subsequent IC), in order to prepare the data for the subsequent feature extraction step. From each stride, stride time,

stance time, and swing time were computed as $IC_i - IC_{i-1}$, $FC_i - IC_i$, and $IC_i - FC_{i-1}$. In addition, 7 temporal-domain features and 6 spectral-domain features were extracted from all components of all inertial signals, as reported in Tab. II. The final feature set was made of 120 features, considering 3 inertial signals (i.e. acceleration, angular velocity, orientation), with 3 components each (i.e. x,y,z). The spectral features were computed from the Fast Fourier Transform (FFT) of the signal. The number of points N_{FFT} in which to represent the FFT was computed as in (1), where \bar{T}_{stride} is the average stride time of PDPs [20] and F_s is the sample frequency. The Shannon entropy E_x of the signal x was computed as in (2).

$$N_{FFT} = \bar{T}_{stride} \cdot F_s \quad (1)$$

$$E_x = x \log(x + \epsilon), \epsilon = 10^{-5} \quad (2)$$

TABLE II
FEATURES EMPLOYED IN THE PRESENT STUDY.

ID	Feature	Description
1	Min	minimum value
2	Max	maximum value
3	Mean	average value
4	Range	range of values
5	Std	standard deviation
6	RMS	root mean square value
7	Entropy	Shannon entropy
8	DH_f	frequency value of the dominant harmonic
9	DH_h	amplitude of the dominant harmonic
10	DH_w	width of the dominant harmonic
11	E_{tot}	total signal energy
12	DH_r	energy in the dominant harmonic divided by E_{tot}
13	Entropy	Shannon entropy of the signal FFT

D. Prediction model

Training-test split. The initial feature set was divided in training and test set, according to the leave-one-subject-out (LOSO) test. It consists in iteratively training the model with data from all subjects except one, which is used for testing purposes. At each iteration of LOSO, the following processing steps were performed.

Normalization. Training and test set were normalized using the range normalization formula reported in (3). Each feature (X) from the training and test set was normalized according to the minimum and maximum value of that feature in the training set.

$$X' = \frac{X - \min(X_{train})}{\max(X_{train}) - \min(X_{train})} \quad (3)$$

Dimensionality reduction. Pearson correlation coefficient (r) of features from the training set was used to discard redundant and non-significant features from both the training and the test set. More specifically, features were discarded if highly correlated with other features ($r > 0.9$) and/or poorly correlated with the target AIM ($r < 0.4$).

Feature selection. The F-test was used to rank features in descending order of importance. The number of selected

features (n_f) was tuned in the range $1-N_f$, where N_f is the total number of features.

Regression model. A random forest regression model was implemented in this study. It is a supervised ML algorithm which averages predictions from multiple decision trees to compute the final output. The number of learners (n_l) is an internal parameter to optimize. Additional parameters to adjust include minimum leaf size (m_{ls}), maximum number of splits (m_{ns}), and maximum parent size (m_{ps}). During the optimization procedure, n_l was tuned in the range 3-40, m_{ls} in 1-30, m_{ns} in 1-20, and m_{ps} in 1-20.

Validation. A k-fold cross validation (CV) was implemented. It consists in dividing the training set into k folds; then, the model is iteratively trained using $k-1$ folds and validated on the remaining fold. The procedure is performed k times, to collect predictions from the entire training set. Data from a given PDP was included either in the training or in the validation set, in order to guarantee subject independence. In this study, k was set to 10, resulting in data from 3 PDPs in each validation fold.

Optimization. A grid search approach was used to optimize the number of selected features and the model parameters. For each combination of n_f , n_l , m_{ls} , m_{ns} , and m_{ps} , 10-fold CV was performed, and root mean square error (RMSE) was computed using predictions from the validation set. The optimal parameters combination was identified searching for the minimum RMSE value.

E. Performance evaluation

Model performance were evaluated using LOSO test. First, given that different observations (corresponding to different strides) from each PDP were available, they were averaged in order to obtain a single measure for each PDP.

Performance were evaluated using the following metrics: Pearson correlation coefficient (r) and the respective p-value, RMSE, and mean absolute error (MAE). The metrics were computed as in (4), (5), and (6), where y_i is the i^{th} label, \hat{y}_i is the i^{th} prediction, and \bar{y} is the average value of labels. Moreover, the correlation plot was obtained from PDPs OFF and ON therapy.

$$r = \sqrt{1 - \frac{\sum_{i=1}^N (y_i - \hat{y}_i)^2}{\sum_{i=1}^N (y_i - \bar{y})^2}} \quad (4)$$

$$RMSE = \sqrt{\frac{1}{N} \sum_{i=1}^N (y_i - \hat{y}_i)^2} \quad (5)$$

$$MAE = \frac{1}{N} \sum_{i=1}^N |y_i - \hat{y}_i| \quad (6)$$

III. RESULTS AND DISCUSSION

Tab. III reports the performance of the proposed prediction model, in terms of the Pearson correlation coefficient with the AIM (i.e. the sum of UPDRS items 2.11-2.13), in patients OFF and ON therapy.

The model provided better performance in PDPs OFF therapy, as evident from all the performance evaluation metrics. The Wilcoxon test demonstrated that predictions were significantly different in PDPs OFF and ON therapy ($p = 0.014$). Fig. 2 reports the correlation plot for PDPs OFF and ON therapy. The equation of the best fit line is provided, together with the Pearson correlation coefficient and the sample size. Larger correlation and smaller prediction errors can be observed in PDPs OFF therapy.

TABLE III
PEARSON CORRELATION COEFFICIENT OF THE PREDICTION MODEL WITH AIM (SUM OF UPDRS ITEMS 2.11-2.13), IN PDPs UNDER (ON) AND NOT UNDER (OFF) DOPAMINERGIC THERAPY. RMSE: ROOT MEAN SQUARE ERROR. MAE: MEAN ABSOLUTE ERROR.

Therapy	r (p)	RMSE	MAE
OFF	0.86 (<0.001)	1.72	1.52
ON	0.76 (<0.001)	2.30	1.70

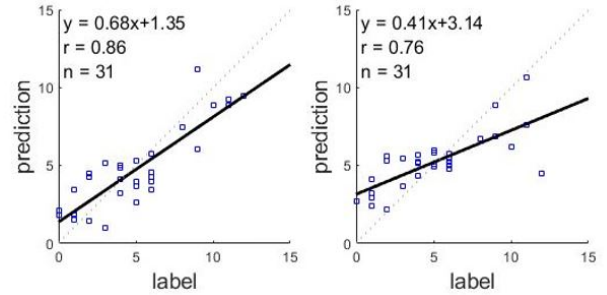


Fig. 2. Correlation plot for PDPs OFF (left) and ON (right) therapy.

Tab. IV reports the Pearson correlation coefficient and the respective p-value for other prediction-clinical score pairs, in PDPs OFF and ON therapy. The predicted score showed moderate to strong correlation with disease progression (measured by the H&Y score), level of clinically evaluated motor impairment (measured by the total UPDRS-III score), and axial impairment (measured by the PIGD score). Again, larger correlations can be observed for PDPs OFF therapy.

TABLE IV
CORRELATION BETWEEN PREDICTION AND VARIOUS CLINICAL SCORES, FOR PDPs OFF AND ON THERAPY. H&Y: HOEHN AND YAHR SCALE. PIGD: POSTURAL STABILITY AND GAIT DIFFICULTY SCORE.

Clinical score	r (p-value)	
	OFF	ON
H&Y	0.68 (<0.001)	0.48 (0.007)
UPDRS-III	0.58 (<0.001)	0.53 (0.002)
PIGD	0.79 (<0.001)	0.69 (<0.001)

Tab. V reports the final feature set used by the prediction model for PDPs OFF and ON therapy. As can be observed, features selected in PDPs ON therapy are a subset of those used for PDPs OFF therapy. As the AIM worsens, minimum and average value of inertial signals increase while movement intensity (measured by the standard deviation) and the signal

energy (measured by the total energy and the amplitude of the dominant harmonic) decrease.

TABLE V

FEATURE SELECTED IN THE OPTIMIZATION PROCEDURE, FOR PATIENTS OFF AND ON THERAPY. α : ACCELERATION; ω : ANGULAR VELOCITY; θ : ORIENTATION

Feature	Component		Trend
	OFF	ON	
Min	ω_x, θ_x	θ_x	increase
Mean	ω_x	-	increase
Std	$\alpha_y, \alpha_z, \omega_x, \omega_y, \theta_x$	ω_x	decrease
DH _h	$\alpha_y, \alpha_z, \omega_y, \omega_x$	ω_x	decrease
E _{tot}	α_z, ω_x	ω_x	decrease

It is worth noting that the regression model was trained and validated to predict the sum of UPDRS items 2.11-2.13. In addition to demonstrating very good prediction capability on such metric, which represents the subjective perception of motor impairment during the preceding days, the algorithm's output correlated with important clinical items. When comparing the present results with that of [16], larger correlation with total MDS-UPDRS part-III ($r = 0.58$ and $r = 0.53$ in PDPs OFF and ON therapy vs $r = 0.48$) and with PIGD score ($r = 0.79$ and $r = 0.69$ in PDPs OFF and ON therapy vs $r = 0.61$) were obtained in this study. Moreover, while in [16] data from 3 sensors recorded during different activities (i.e. gait, turn, stance) were analyzed, in this study only gait data recorded using a single sensor were processed. Compared to [17], correlation with PIGD is equal in patients OFF therapy, while a lower correlation is observed in patients ON therapy ($r = 0.69$ vs $r = 0.75$). However, we remark that the proposed algorithm was not developed for PIGD prediction, as this does not represent the main goal of this study.

IV. CONCLUSION AND FUTURE WORK

In this work, 31 patients affected by Parkinson's disease were enrolled. Standardised scales (H&Y, MDS-UPDRS part II and part III, PIGD score) were used to assess their axial impairment, postural instability, and gait difficulties during daily activities. All the PDPs performed the same tests wearing a single IMU on the thigh and correlations between inertial data and scale scores were analyzed in both OFF and ON state of therapy using regression algorithms. A set of 120 features was extracted and divided into training and test sets according to a LOSO test. Both feature selection and regression model parameters were optimized. As a result, the model provided large prediction correlations in the whole cohort of patients for all the investigated scores, with larger values and smaller errors in PDPs OFF therapy.

ACKNOWLEDGMENT

Authors wish to thank Alessandro Gumiero and Luigi Della Torre from STMicroelectronics (Agrate Brianza, Italy) for providing nMEMSi devices.

REFERENCES

- [1] A. Samii, JG. Nutt, BR. Ransom, "Parkinson's disease," Lancet, vol. 363, pp. 1783–1793, 2004.
- [2] M. Armstrong, M. Okun, "Diagnosis and Treatment of Parkinson Disease: A Review," JAMA, vol. 60, pp. 323-548, 2020.
- [3] F. Magrinelli, A. Picelli, P. Tocco, A. Federico et al, "Pathophysiology of Motor Dysfunction in Parkinson's Disease as the Rationale for Drug Treatment and Rehabilitation," Park. Dis, 2016.
- [4] J. Jankovic, "Parkinson's disease: clinical features and diagnosis," J Neurol. Neurosurg. Psychiatry, vol. 79 (4), pp. 368–376, 2008.
- [5] CG. Goetz et al, "Movement disorder society-sponsored revision of the unified Parkinson's disease rating scale (MDS-UPDRS): scale presentation and clinimetric testing results," Mov. Disord., vol. 23 (15), pp. 2129–2170, 2008.
- [6] L. Borzi, S. Fornara, F. Amato, G. Olmo et al, "Smartphone-based evaluation of postural stability in Parkinson's disease patients during quiet stance, Electronics, vol.9, pp. 919, 2020.
- [7] H. Dai, G. Cai, Z. Lin, Z. Wang and Q. Ye, "Validation of inertial sensing-based wearable device for tremor and bradykinesia quantification," IEEE Journal of Biomedical and Health Informatics, vol. 25 (4), pp. 997-1005, 2021.
- [8] MD. Hssayeni, J. Jimenez-Shahed, MA. Burack and B. Ghoraani, "Dyskinesia severity estimation in patients with Parkinson's disease using wearable sensors and a deep LSTM network," 42th Annual International Conference of the IEEE Engineering in Medicine Biology Society (EMBC), pp. 6001-6004, 2020.
- [9] L. Sigcha, I. Pavón, N. Costa, S. Costa et al, "Automatic Resting Tremor Assessment in Parkinson's Disease Using Smartwatches and Multitask Convolutional Neural Networks", Sensors, vol. 21 (1), pp. 291, 2021.
- [10] L. Borzi, G. Olmo, CA. Artusi and L. Lopiano, "Detection of freezing of gait in people with Parkinson's disease using smartphones," IEEE 44th Annual Computers, Software, and Applications Conference (COMPSAC), pp. 625-635, 2020.
- [11] A. Suppa, A. Kita et al, "1-DOPA and freezing of gait in Parkinson's disease: objective assessment through a wearable wireless system," Frontiers in Neurology, vol. 8, pp. 406, 2017.
- [12] F. Parisi et al., "Body-sensor-network-based kinematic characterization and comparative outlook of UPDRS scoring in leg agility, sit-to-stand, and gait tasks in Parkinson's disease," IEEE Journal of Biomedical and Health Informatics, vol. 19 (6) pp. 1777–1793, 2015.
- [13] L. Borzi, G. Olmo, CA. Artusi, M. Fabbri et al, "A new index to assess turning quality and postural stability in patients with Parkinson's disease," Biomedical Signal Processing and Control, vol. 62, 2020.
- [14] A. Rodríguez-Molinero, A. Samà, C. Pérez-López, D. Rodríguez-Martín et al, "Analysis of correlation between an accelerometer-based algorithm for detecting parkinsonian gait and UPDRS subscales," Frontiers in Neurology, vol.8, pp. 431, 2017.
- [15] L. Borzi, M. Varrecchia, S. Sibille, G. Olmo et al, "Smartphone-based estimation of item 3.8 of the MDS-UPDRS-III for assessing leg agility in people with Parkinson's disease," IEEE Open Journal of Engineering in Medicine and Biology, vol. 1, pp. 140-147, 2020.
- [16] D. Safarpour, ML. Dale, VV. Shah, L. Talman et al, "Surrogates for rigidity and PIGD MDS-UPDRS subscores using wearable sensors," Gait Posture, vol. 91, pp. 186-191, 2022.
- [17] L. Borzi, I. Mazzetta, A. Zampogna, A. Suppa, F. Irrera, G. Olmo, "Predicting Axial Impairment in Parkinson's Disease through a Single Inertial Sensor, Sensors, vol. 22, pp. 412, 2022
- [18] D. Comotti, M. Galizzi, A. Vitali, "One step forward in wireless attitude and heading reference systems," 2014 International Symposium on Inertial Sensors and Systems (ISISS), pp. 1-4, 2014.
- [19] M. Caruso, A.M. Sabatini, D. Laidig, T. Seel, M. Knafitz, U. Croce, A. Cereatti, "Analysis of the Accuracy of Ten Algorithms for Orientation Estimation Using Inertial and Magnetic Sensing under Optimal Conditions: One Size Does Not Fit All," Sensors, vol. 21, pp. 2543.
- [20] R. Bouça-Machado, C. Jalles, D. Guerreiro, F. Pona-Ferreira et al, "Gait Kinematic Parameters in Parkinson's Disease: A Systematic Review," Journal of Parkinson's Disease, vol. 10, pp. 843–853, 2020.
- [21] N. Abhayasinghe, I. Murray, "Human gait phase recognition based on thigh movement computed using IMUs," IEEE 9th International Conference on Intelligent Sensors, Sensor Networks and Information Processing (ISSNIP), pp. 1-4, 2014.